Hydrophobic moments of protein structures: Spatially profiling the distribution

B. David Silverman*

IBM Thomas J. Watson Research Center, P.O. Box 218, Yorktown Heights, NY 10598

It is generally accepted that globular proteins fold with a hydrophobic core and a hydrophilic exterior. Might the spatial distribution of amino acid hydrophobicity exhibit common features? The hydrophobic profile detailing this distribution from the protein interior to exterior has been examined for 30 relatively diverse structures obtained from the Protein Data Bank, for 3 proteins of the 30S ribosomal subunit, and for a simple set of 14 decoys. A second-order hydrophobic moment has provided a simple measure of the spatial variation. Shapes of the calculated spatial profiles of all native structures have been found to be comparable. Consequently, profile shapes as well as particular profile features should assist in validating predicted protein structures and in discriminating between different protein-folding pathways. The spatial profiles of the 14 decoys are clearly distinguished from the profiles of their native structures.

second-order moment | quasiinvariant | hydrophobic ratio

It is generally observed and accepted that globular proteins involve a spatial transition between a hydrophobic core and a hydrophilic exterior (1). Might a detailed characterization of this transition reveal common features? The present paper describes such characterization and identifies two features that are essentially comparable for all of the native structures examined. One is the overall shape or profile of the second-order ellipsoidal hydrophobic moment calculated from protein interior to exterior. The other is a simple ratio of distances at which the second- and zero-order moments of the amino acid distribution of hydrophobicity vanish. Perhaps it should be no surprise that the transition from hydrophobic interior to hydrophilic exterior exhibits spatial characteristics that are common to many, if not to most, globular proteins. The interaction of the amino acid residues of varying hydrophobic attributes with the aqueous environment assists in the selection of the folding pathway that leads to the final protein structure.

The spatial variation of hydrophobicity has been calculated by a second-order ellipsoidal moment utilizing the hydrophobicity consensus scale of Eisenberg (2). Table 1 lists the values assigned to each of the amino acid residues. The hydrophobic moment (2, 3), a first-order moment, has provided a useful measure of the amphiphilicity of α-helical structures. Whereas the first-order moment provides a measure of amphiphilicity, the second-order moment enables the spatial profiling of protein hydrophobicity. The spatial variation arises simply from the spatial distribution of amino acid residues.

Protein structures can be approximated by all sorts of geometric shapes: spherical, ellipsoidal, cylindrical, conical, and other. Because this paper focuses on globular proteins, an ellipsoidal representation of shape will be used. The centroid of the spatial distribution of amino acid residue centroids provides an origin for the moment expansion. It will be shown that shifting the Eisenberg consensus scale of amino acid hydrophobicity such that the net value of protein hydrophobicity vanishes yields a second-order moment profile and hydrophobic ratio that are comparable for all the native structures examined. These features should assist in validating predicted tertiary protein structures and in discriminating between different protein-folding pathways.

A second-order hydrophobic moment had been previously proposed in connection with the description of protein hydrophobicity (2). A second-order moment, the electrostatic quadrupole, has been used as a molecular descriptor for drug discovery (4).

The paper is organized as follows:

A Two-Component Spherical Model treats an idealistic representation of the spatial transition of hydrophobicity from the interior to the exterior of a protein. It illustrates, in a transparent manner, several of the underlying features as well as the rationale of the detailed calculations. *Molecular Moments and Hydrophobicity Profiling* reviews several aspects of moment expansions relevant for the present calculations and provides a description of the computational procedure. *Results of Profiling the Structures* presents the results. *Conclusions* is a summary and discussion of the results.

A Two-Component Spherical Model

The following idealized simple two-component representation of protein hydrophobicity, although deficient in several respects, provides a simple frame of reference in the attempt to understand the regularities found by the detailed calculations presented in the next two sections. The simple model yields the two features alluded to in the Introduction that were found to be comparable for the native structures. It also suggests the interesting possibility of encapsulating the detailed results within the context of a two-component model. Even though this model is not used for the computational procedures described in the following sections, it clearly illustrates the objectives of these calculations within a simpler context.

Let us assume the protein to be represented by a sphere of radius R_S. We further assume that two components, hydrophobic and hydrophilic, are distributed over the sphere. For example, residues with positive consensus value might be coalesced into a hydrophobic component, whereas residues of negative value might be coalesced into a hydrophilic component.

If the density of hydrophobicity, $\rho(r)$, at r, a radial distance from the center of the sphere, is assumed to be

$$\rho(r) = \alpha r^\eta - \beta r^\mu \quad 0 \le r \le R_S, \quad [1]$$

the hydrophobic component will contribute an amount, $4\pi\alpha r^\eta r^2 dr$ in a shell of width dr, and the hydrophilic component an amount $-4\pi\beta r^\mu r^2 dr$.

At a distance, $R \le R_S$ from the center of the sphere, the accumulated hydrophobicity or zero-order moment, T_0, of the distribution will be

Table 1. Eisenberg hydrophobicity consensus scale

Residue	Consensus value
Arginine	−1.76
Lysine	−1.10
Aspartic acid	−0.72
Glutamine	−0.69
Asparagine	−0.64
Glutamic acid	−0.62
Histidine	−0.40
Serine	−0.26
Threonine	−0.18
Proline	−0.07
Tyrosine	0.02
Cysteine	0.04
Glycine	0.16
Alanine	0.25
Methionine	0.26
Tryptophan	0.37
Leucine	0.53
Valine	0.54
Phenylalanine	0.61
Isoleucine	0.73

$$T_0 = 4\pi \int_0^R (\alpha r^\eta - \beta r^\mu) r^2 dr = T_0^a + T_0^b = \frac{aR^{n+1}}{n+1} - \frac{bR^{m+1}}{m+1},$$
[2]

and the second-order radial moment will be

$$T_2 = 4\pi \int_0^R (\alpha r^\eta - \beta r^\mu) r^4 dr = T_2^a + T_2^b = \frac{aR^{n+3}}{n+3} - \frac{bR^{m+3}}{m+3},$$
[3]

where $a = 4\pi\alpha$, $n = \eta + 2$ and $b = 4\pi\beta$, $m = \mu + 2$.

We further assume that $n < m$ and $a, b > 0$. Therefore, at small radial distances, the hydrophobic component prevails, and T_0 and T_2 are positive. As the distance from the origin increases, T_2 will change sign before T_0 goes to zero. We further assume that T_0 vanishes at R_S, the surface of the sphere, and that T_2 vanishes at R_2.

From Eqs. 2 and 3, these distances are

$$R_S^{m-n} = \left(\frac{a}{b}\right)\left(\frac{m+1}{n+1}\right)$$
[4]

$$R_2^{m-n} = \left(\frac{a}{b}\right)\left(\frac{m+3}{n+3}\right).$$
[5]

Their ratio is given by

$$Rt^{m-n} = \frac{R_2^{m-n}}{R_S^{m-n}} = \frac{(m+3)(n+1)}{(m+1)(n+3)} < 1.$$
[6]

Rt^{m-n} can also be obtained by

$$Rt^{m-n} = (T_2^a/T_0^a)/(T_2^b/T_0^b) = \frac{(m+3)(n+1)}{(m+1)(n+3)} \quad 0 \leq R \leq R_S.$$
[7]

The ratio Rt^{m-n} extracts the powers of the algebraic distribution of Eq. 1 and does not depend on the prefactors.

The spatial profiles of the moments T_0 and T_2 are illustrated as a function of R in Fig. 1. The second-order moment, T_2, increases as the hydrophobic region is traversed. As the more
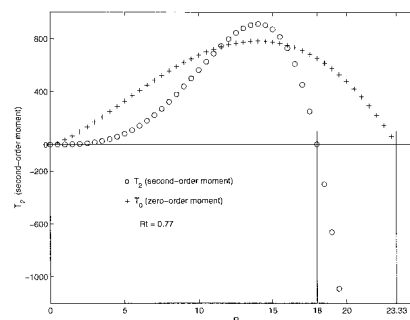

Fig. 1. The zero- and second-order moments, T_0 and T_2, plotted as a function of R. The prefactors of T_0 have been multiplied by a factor of 40 to place it on the same vertical scale of values shown for T_2. The values chosen are $n = 0.5$, $m = 1.5$, and $b = 1$. The zero crossing of T_2 has been arbitrarily placed at $R = 18$. $Rt = 0.77$.

hydrophilic region is entered and then traversed, the increase initially slows and then plunges through zero to negative values.

Profiles of the second-order hydrophobic moment for all native structures, calculated by the procedure described in the next section, approximate the profile shape shown in Fig. 1. Zero crossings of this moment can, therefore, be identified for each of the structures. The calculated range of values of the hydrophobic ratio, Rt, for all of the 30 structures is comparable to the range of values, 0.67 and 0.83, obtained by the two-component model for the values of $m = 1$, $n = 0$, and $m = 2$, $n = 1$, respectively.

Molecular Moments and Hydrophobicity Profiling

The zero- and first-order moments of the amino acid distribution of protein hydrophobicity are

$$H_0 = \sum_i h_i$$
[8]

$$\vec{H}_1 = \sum_i h_i \vec{r}_i$$
[9]

$\vec{r}_i$ is a vector to the centroid of the ith amino acid residue with hydrophobicity consensus value h_i. The sum is over all n amino acid residues.

Because the zero-order moment, H_0, or net hydrophobicity of the protein, is generally nonvanishing, the first-order moment will depend on the origin of the calculation. In connection with the calculated moments of α helices, Eisenberg et al. (2, 3) had pointed out that the first-order moment would be invariant if hydrophobicity differences about the mean, $\bar{h}$, were calculated with respect to an arbitrary origin,

$$\vec{H}_1 = \sum_i (h_i - \bar{h})\vec{r}_i$$
[10]

with, $\bar{h} = H_0/n$. Using the protein centroid as the origin of the moment expansion yields this invariant value of the first-order moment, namely,

$$\vec{H}_1 = \sum_i h_i(\vec{r}_i - \vec{r}_c)$$
[11]

$$\vec{r}_c = (1/n)\sum_i \vec{r}_i$$
[12]

The first-order moment calculated about the centroid of the protein is, therefore, a measure of first-order hydrophobic imbalance about the mean. With the inclusion of values of the solvent-accessible surface area, s_i, for each of the residues, the

surface-exposed first-order hydrophobic moment imbalance about the entire protein can then be written,

$$\bar{H}_1^s = \sum_i h_i s_i (\vec{r}_i - \vec{r}_c). \qquad [13]$$

This moment could provide useful information with respect to the three-dimensional spatial affinity of the tertiary protein structure and external structures with which it might interact.

Second-order moments provide the capability of spatially profiling the hydrophobicity distribution of amino acid residues. This is the primary focus of the present paper. Proteins come with all sorts of overall shape. *A Two-Component Spherical Model* used a spherical representation of shape. A representation that is the simplest generalization of this ideal shape is an ellipsoidal representation. This shape can be generated from the molecular moments of geometry, i.e., moments of inertia for which all amino acid residue centroids are weighted by unity instead of by residue mass. The calculation is performed with the centroid of the amino acid centroids of the protein as origin. The moments of geometry are designated g_1, g_2, and g_3, with $g_1 < g_2 < g_3$. The ellipsoidal representation generated by these moments is written as

$$x^2 + g_2' y^2 + g_3' z^2 = d^2, \qquad [14]$$

with $g_2' = g_2/g_1$, $g_3' = g_3/g_1$. The coordinates x, y, and z are written in the frame of the principal geometric axes.

The ellipsoidal surface obtained by the choice of a particular value of d enables the collection of the values of hydrophobicity for all amino acid residues of number n_d lying within this surface. The consensus hydrophobicity scale of Table 1 has been used in all of the calculations. The distribution of amino acid hydrophobicity is, however, shifted such that the net hydrophobicity of each protein vanishes. The distribution is then normalized to yield a standard deviation of 1. Such shifting of the values of amino acid hydrophobicity eliminates the zero-order moment from the distribution and consequently the dependence of the second-order moment on differences in net protein hydrophobicity. This scaling provides a basis for comparison of the hydrophobic moment profiles of the different proteins and consequently a basis for comparison of their hydrophobic ratios.

The average hydrophobicity per residue collected within the ellipsoidal surface specified by d is then written,

$$H_0^d(d) = (1/n_d) \sum_{i \le d} h_i' = (1/n_d) \sum_{i \le d} (h_i - \bar{h}) / \langle (h_j - \bar{h})^2 \rangle^{1/2}. \qquad [15]$$

The superscript d indicates that the moment has been divided by the number of residues. The prime designates the value of hydrophobicity of each residue after shifting and normalizing the distribution. When the value of d is just large enough to collect all of the residues, the net hydrophobicity of the protein vanishes. This value of d assigns a "protein surface" as a location of common reference. Calculations performed for each of the proteins will examine increasing the value of d until all residues have been collected and the mean hydrophobicity vanishes.

The value of the second-order ellipsoidal moment per residue from residues lying within the ellipsoidal surface specified by d is written

$$H_2^d(d) = (1/n_d) \sum_{i \le d} h_i'(x_i^2 + g_2' y_i^2 + g_3' z_i^2) = (1/n_d) \sum_{i \le d} h_i' d_i^2. \qquad [16]$$

When all residues fall within the ellipsoidal surface and are collected, one finds:

Table 2. Protein structures profiled and number of residues

PDB ID	Number	PDB ID	Number
1ORC	63	1BN1c	257
1CDZ	96	2DRI	271
1NEU	115	1AUA	296
1DZOc	120	1LDM	329
1A4V	123	1FSZ	334
1AT0	125	1UBY	348
1PDO	129	1A26	351
2SNS	141	1PHC	405
1CQ2c	153	1BGV	449
1PHR	154	3PBG	468
1CTQ	166	1GAIc	472
121P	166	3COXc	500
1DZV	206	1FEH	574
1AUN	208	B_1FJFc	234
1LBU	213	C_1FJFc	206
2ACT	218	D_1FJFc	208
1AKZ	223		

The superscript c indicates that hydrophobicity assignments have been made at the α-carbon locations; all others are made at the centroid of the amino acid residue.

$$H_2^d = (1/n) \sum_i h_i' d_i^2 = (1/n) \sum_i (h_i / \langle (h_j - \bar{h}^2) \rangle^{1/2})(d_i^2 - \bar{d}^2), \qquad [17]$$

where

$$\bar{d}^2 = (1/n) \sum_i d_i^2. \qquad [18]$$

The values of $H_0^d(d)$ and $H_2^d(d)$ are calculated for each protein with increasing values of d, and the ratio $Rt = d_-/d_0$ obtained. d_- is the value of d for which $H_2^d(d)$ has changed sign, becoming negative, and d_0 the value for which $H_0^d(d)$ vanishes. We have adopted the protocol that for d_- to be chosen, all values of $H_2^d(d)$ at larger values of d must be negative. The ratio, Rt, is what we have called the hydrophobic ratio of distances or just the hydrophobic ratio. The next section will show it to be quasiinvariant or roughly comparable in value for all of the native protein structures examined.

Results of Profiling the Structures

Protein structures were selected by keyword searches of the Protein Data Bank (PDB) and by examination of entries in different SCOP (5) classes. The objective was to choose a selection representative of different sizes and different classes. Thirty protein structures were chosen in this manner. For an internal check, two of the proteins chosen included 1CTQ and 121P, the same protein with independently determined structures. Three additional proteins were also chosen from the recently determined structure of the 30S ribosomal subunit (6). The PDB identification numbers and number of amino acid residues for each are listed in Table 2. Finally, 14 simple decoys as well as their native structures were also chosen for examination (ref. 7; I am indebted to Richard Friesner for suggesting this calculation).

Detailed results of profiling one of the structures, 1AKZ, are shown in Fig. 2 and Table 3. The figure shows the profile of the accumulated zero-order moment, $H_0(d)$, and second-order moment, $H_2(d)$. Table 3 lists the moments per residue, $H_0^d(d)$ and $H_2^d(d)$. As the distance, d, that defines the extent of the ellipsoid is increased, the first residue falls within the ellipsoidal surface at a value of d equal to 4 Å. From Fig. 2, one sees the
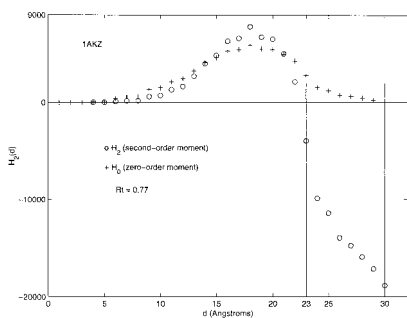
Fig. 2. The zero- and second-order ellipsoidal moment profiles of the protein 1AKZ. The zero-order moments have been multiplied by a factor of 120 to place them on the same vertical scale of values shown for the second-order moment.

Fig. 3. A view along one of the principal axes of 1AKZ. The interior, intermediate, and exterior contours are drawn at the maximum value of H_2, $d = 16$, and for $d_- = 23$, $d_0 = 30$.

second-order moment increase in value until it turns around rapidly, becoming negative. At the 1-Å resolution of the calculation shown in Table 3, the first negative value appears at $d_- = 23$. The hydrophobicity, $H_0^d(d)$, of the protein becomes zero at $d_0 = 30$. Rt, the hydrophobic ratio, has a value, therefore, of $23/30 = 0.77$. One notes that the second-order moment profile of Fig. 2 has a similar shape to the second-order moment profile shown in Fig. 1, the profile obtained for the idealized two-component model. The steep decrease of the more realistic ellipsoidal model tapers off, however, in the final range of 25–30 Å. Both zero- and second-order moments peak at the same value of d, and this distance, at which the maximum occurs, can also be used as a feature for comparison between different proteins.

Fig. 3 shows a view along one of the three principal axes of 1AKZ. The projections of the amino acid centroids have been plotted as well as the elliptical boundaries in the plane containing two of the principal axes. The ellipses have been plotted for the
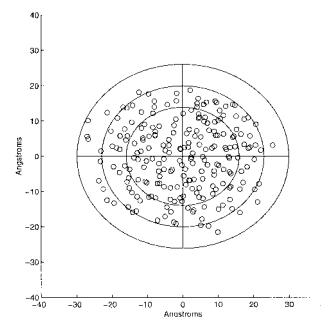
value $d = 16$, where the second-order moment is greatest, the value of $d_- = 23$, the value at which H_2 has just changed sign, and the value $d_0 = 30$, the value for which all amino acid residue centroids fall just within the ellipsoidal surface, the protein hydrophobicity vanishing. The region of increasing H_2 reflects the predominance of the spatial distribution of residues comprising the hydrophobic core. At larger d, the slowing of this increase and plunge to negative values reflect the spatially increasing prevalence of hydrophilic residues. Such regular behavior is required for the identification of d_- and consequently for the calculation of Rt. Keeping the 1AKZ structure fixed and randomly shuffling the hydrophobicity values among the different residues yields the results shown in Table 4. It is evident from examination of this table that a value of d_- cannot be assigned from this distribution of values of the second-order moment.

Table 3. Zero and second-order moments of 1AKZ

d (Angstroms)	n_d	$H_0^d(d)$	$H_2^d(d)$
4	1	0.288	2.62
5	1	0.288	2.62
6	5	0.607	16.86
7	7	0.657	22.28
8	7	0.657	22.28
9	13	0.842	45.1
10	16	0.779	44.53
11	24	0.738	54.44
12	27	0.75	60.8
13	40	0.675	67.57
14	53	0.645	75.13
15	63	0.606	76.76
16	77	0.574	81.75
17	89	0.51	74.23
18	101	0.487	77.2
19	114	0.403	58.94
20	138	0.328	47.12
21	156	0.266	32.14
22	168	0.211	12.68
23	184	0.127	−21.54
24	200	0.063	−49.53
25	208	0.048	−54.96
26	215	0.029	−64.99
27	218	0.023	−67.81
28	220	0.016	−72.45
29	221	0.008	−77.65
30	223	0	−84.67

Table 4. Zero and second-order moments for a random residue distribution of 1AKZ

d (Angstroms)	n_d	$H_0^d(d)$	$H_2^d(d)$
4	1	−0.421	−3.84
5	1	−0.421	−3.84
6	5	−0.486	−13.50
7	7	−0.518	−17.11
8	7	−0.518	−17.11
9	13	−0.238	−6.41
10	16	−0.187	−3.92
11	24	−0.025	8.41
12	27	0.011	11.64
13	40	0.041	12.76
14	53	0.040	10.66
15	63	0.058	14.02
16	77	−0.074	−17.48
17	89	−0.003	1.23
18	101	−0.008	−0.24
19	114	−0.024	−5.92
20	138	−0.021	−4.35
21	156	−0.009	−0.19
22	168	−0.008	−0.19
23	184	0.004	5.15
24	200	0.009	7.99
25	208	0.018	13.58
26	215	0.034	23.84
27	218	0.024	16.36
28	220	0.015	10.03
29	221	0.011	6.64
30	223	0.000	−2.56
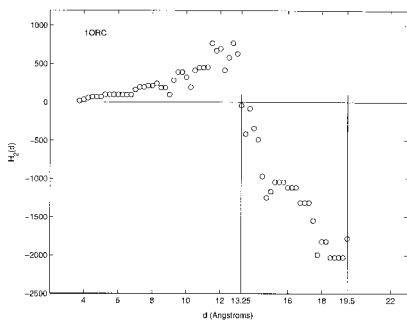
Fig. 4. The second-order ellipsoidal moment profile of the protein 1ORC.

Fig. 6. A view along one of the principal axes of 1LDM showing the contour at $d = 37$, which truncates the arm of the protein.

Figs. 4 and 5 show the second-order ellipsoidal moment profiles obtained for the smallest protein, 1ORC, and the largest, 1FEH. 1ORC has been profiled with a resolution of 0.25 Å in Fig. 4. At this resolution, $Rt = 0.68$. Even though the scales of the axes of both figures differ significantly, the overall profile shapes over the extent of the proteins are similar. Again, there is an initial increase in the value of the second-order moment before plunging to negative values. The hydrophobic ratios, Rt, of 1ORC and 1FEH are 0.70 and 0.71, respectively, for the 1-Å resolution used to obtain the entries listed in Table 5. These two examples highlight the relative independence of the overall second-order moment profile shape and hydrophobic ratio with respect to differences in protein size.

All 30 protein structures exhibit similar spatial behavior for either the accumulated second-order hydrophobic moment, $H_2(d)$, or $H_2^d(d)$, the moment per residue. The accumulated profiles are, however, somewhat smoother and accentuate the plunge to negative values as the surface of the protein is approached. The results for the 30 protein structures and 3 ribosomal proteins are published as supplemental data on the PNAS web site, www.pnas.org. Table 5 lists the value of the hydrophobic ratio for each of the protein structures. All 30 structures yield a mean value of the ratio equal to 0.75, with a standard deviation of 0.045. The numerator and denominator of Rt, d_- and d_0, are also listed. This clearly shows how d_- increases with increasing protein size to provide comparable values of the ratio for all 30 proteins. The value of d_0 scales roughly as a factor of two between the largest and smallest proteins examined. This increase in d_0 is as expected, because the ratio of the number of amino acid residues of the largest to smallest protein structures is approximately equal to $600/70$, and consequently $(600/70)^{1/3} \approx 2$. d_0 can be considered an approximate measure of the linear extent of the protein. Consequently, the values of d_- are then equal to a comparable fraction of the extent of each of the proteins, for all of the structures.

Table 5 also shows the results of profiling the distribution with a spherical instead of ellipsoidal contour. The crossover between
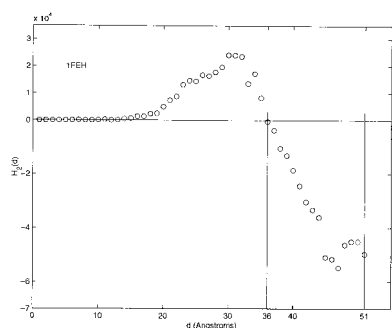

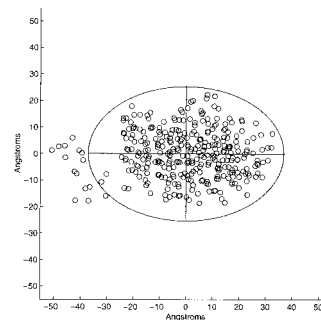**Fig. 5.** The second-order ellipsoidal moment profile of the protein 1FEH.

the positive and negative values of H_2 is still well defined. Consequently, a value for the hydrophobic ratio, Rt, can be calculated. One notes its greater variability with spherical profiling.

A few of the proteins require special attention. Three of the structures, 1PDO, 1LDM, and 1FSZ, have extended arms that are away from the main body of the protein. Collecting all residues to determine the value of d_0 yields a value that is not representative of the protein bulk. Shifting the scale of residue hydrophobicity such that the net hydrophobicity of the protein is zero when all residues of the bulk are collected yields the values given in Table 5. Fig. 6 shows a view along one of the principal axes of 1LDM with the ellipsoidal intercept in the plane of the two other principal axes. The intercept has been drawn for the value $d = 37$, a value that does not include the contribution from the structural arm.

Structure 1LBU exhibits slightly deviant behavior of H_2. There is a rapid crossover to a negative value of the second-order moment at a value of d equal to 20. This value remains negative until, at $d = 23$, it becomes marginally positive before becoming negative again at $d = 24$ and thereafter. The two zero crossovers at $d = 20$ and $d = 24$ yield a hydrophobic-ratio average of 0.76.

Two of the ribosomal proteins, B_1FJF (chain B; protein S2) and D_1FJF (chain D; protein S4), are the largest deviants with respect to the values of Rt for the nonribosomal proteins. On the other hand, C_1FJF (chain C; protein S3) yields a value of Rt that is within the range of the other 30 values. C_1FJF makes no contact with RNA at all and exhibits an α/β domain frequently found in different proteins with α helices packed against a β sheet (6).

Finally, ellipsoidal moment profiling has been performed on a simple decoy set (7). Fourteen decoys and native structures of this set, with a number of residues greater than 100, were downloaded from the web (structures were downloaded from http://dd.stanford.edu/download.shtml). Twenty-eight moment calculations were, therefore, performed. A typical result is shown in Fig. 7. Visual inspection of the figure clearly delineates the difference between the correct or native structure and the decoy structure. Figures for all 14 structures look essentially the same. The results for the 28 decoy and native structures are available as supplementary material, www.pnas.org. All native structures exhibit a second-order moment profile similar to what had been obtained for the 30 PDB structures. Consequently, hydrophobic ratios can be calculated, and they span the range of values previously found for the 30. The spatial transition to the hydrophilic exterior of the native structures is significantly amplified by the second-order moment. The decoys do not exhibit this plunge to negative values of the second-order moment, nor is the relatively regular behavior in the protein interior reproduced. Hydrophobic ratios cannot, therefore, be assigned to any of the decoy structures.

Table 5. Hydrophobic ratios of 30 PDB protein structures and 3 ribosomal proteins

PDB ID	d_-/d_0	Rt	Spherical	PDB ID	d_-/d_0	Rt	Spherical
1ORC	14/20	0.70	0.68	1BN1[c]	23/30	0.77	0.72
1CDZ	18/23	0.78	0.73	2DRI	31/37	0.84	0.94
1NEU	18/28	0.64	0.64	1AUA	28/34	0.82	0.79
1DZO[c]	21/29	0.72	0.68	1LDM	30/37	0.81	0.71
1A4V	20/29	0.69	0.63	1FSZ	25/34	0.74	0.70
1AT0	19/25	0.76	0.74	1UBY	30/43	0.70	0.70
1PDO	18/23	0.78	0.70	1A26	29/41	0.71	0.68
2SNS	20/28	0.71	0.63	1PHC	29/38	0.76	0.73
1CQ2[c]	17/25	0.68	0.70	1BGV	30/38	0.79	0.76
1PHR	19/26	0.73	0.69	3PBG	29/37	0.78	0.77
1CTQ	19/25	0.76	0.79	1GAI[c]	27/37	0.73	0.66
121P	19/25	0.76	0.75	3COX[c]	30/38	0.79	0.68
1DZV	26/34	0.76	0.74	1FEH	36/51	0.71	0.63
1AUN	22/29	0.76	0.71	B_1FJF[c]	25/43	0.58	0.49
1LBU	22/29	0.76	0.58	C_1FJF[c]	26/36	0.72	0.73
2ACT	22/28	0.79	0.70	D_1FJF[c]	29/33	0.89	0.81
1AKZ	23/30	0.77	0.72				

Conclusions

This paper has focused on the spatial region of transition between the hydrophobic core and hydrophilic exterior of globular proteins. The moment calculations have identified two features, apparently independent of protein size and fold, that are comparable for the 30 protein structures obtained from the PDB and for the 14 native structures of the decoy set. One, a global feature, is the overall shape or profile of the second-order ellipsoidal moment calculated from protein interior to exterior. The other, a specific feature, the hydrophobic ratio, is the ratio of distances at which the second- and zero-order moments of the distribution vanish. Such correspondence of features over the set of proteins examined had not been initially expected.

Although it might seem surprising that the profile shapes and hydrophobic ratios are comparable over a set of diverse protein sizes and structures, the origin of this correspondence might be inferred by examination of the relative increase of the cumulative hydrophobic and hydrophilic moments with increasing distance from the protein interior. Consequently, the results of the two-component spherical model indicate that, with a power law

Fig. 7. The second-order ellipsoidal profile of the native and decoy structures of 2i1b.

fit to these cumulative increases, this simple model would yield values of the hydrophobic ratio that would be comparable to those obtained by the detailed calculations.

The comparison between the second-order moment profiles of the native with the decoy structures is revealing. The second-order moment amplifies differences about the mean protein hydrophobicity. Profiles of the native structures reflect the significant separation between the hydrophobic residues comprising the core and the hydrophilic residues of the protein exterior. The decoy residue distribution fails to mirror this separation. This suggests that moment profiling should play an important role in recognizing the difference between native and decoy folds. It should also play a role in validating predicted protein structures.

With respect to molecular dynamics and protein-folding pathways, profiling could be done at various points in the folding trajectory. One would then look for trajectories that begin to exhibit a relatively smooth monotonic increase of the second-order moment in the structural interior, with the onset of a transition to negative values near the exterior. It would then be of interest to see how close such identification would appear with respect to the final native structure achieved. After identification or selection of such trajectory, fine tuning could be observed or directed by examination of the hydrophobic ratio. Considering the native structure as the endpoint in the folding trajectory, perhaps the moment regularities will provide not only constraints with respect to the pathways selected but also a clue to the underlying processes responsible for such selection.

To conclude, the procedure described in this paper need not be restricted to examination of globular proteins but can be used in connection with the profiling of proteins of diverse overall structure, with the choice of an appropriate overall profiling geometry.
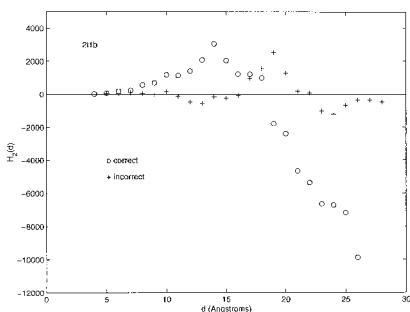
1. Meirovitch, H. & Scheraga, H. A. (1981) *Macromolecules* **14,** 340–345.
2. Eisenberg, D., Weiss, R. M., Terwilliger, T. C. & Wilcox, W. (1982) *Faraday Symp. Chem. Soc.* **17,** 109–120.
3. Eisenberg, D., Weiss, R. M. & Terwilliger, T. C. (1982) *Nature (London)* **299,** 371–374.
4. Silverman, B. D. & Platt, D. E. (1996) *J. Med. Chem.* **39,** 2129–2140.
5. Murzin, A. G., Brenner, S. E., Hubbard, T. & Chothia, C. (1995) *J. Mol. Biol.* **247,** 536–540.
6. Wimberly, B. T., Brodersen, D. E., Clemons, W. M., Jr., Morgan-Warren, R. J., Carter, A. P., Vonrhein, C., Hartsch, T. & Ramakrishnan, V. (2000) *Nature (London)* **407,** 327–339.
7. Holm, L. & Sander, C. (1992) *J. Mol. Biol.* **225,** 93–105.

BIOCHEMISTRY